Selected Papers

Fluorido Complex Formation of Element 104, Rutherfordium (Rf)

Yasuo Ishii,[1,2] Atsushi Toyoshima,*[1] Kazuaki Tsukada,[1] Masato Asai,[1] Zijie Li,[1] Yuichiro Nagame,[1] Sunao Miyashita,[2] Tomotaka Mori,[2] Hideo Suganuma,[2] Hiromitsu Haba,[3] Shin-ichi Goto,[4] Hisaaki Kudo,[4] Kazuhiko Akiyama,[5] Yasuji Oura,[5] Atsushi Shinohara,[6] Matthias Schädel,[1,7] Valeria Pershina,[7] and Jens V. Kratz[8]

[1]Advanced Science Research Center, Japan Atomic Energy Agency (JAEA), Tokai, Ibaraki 319-1195

[2]Radiochemical Research Laboratory, Shizuoka University, Shizuoka 422-8529

[3]Nishina Center for Accelerator-Based Science, RIKEN, Wako, Saitama 351-0198

[4]Department of Chemistry, Niigata University, Niigata 950-2181

[5]Graduate School of Science and Engineering, Tokyo Metropolitan University, Hachioji, Tokyo 192-0397

[6]Graduate School of Science, Osaka University, Toyonaka, Osaka 560-0043

[7]GSI Helmholtzzentrum für Schwerionenforschung GmbH, D-64291 Darmstadt, Germany

[8]Institut für Kernchemie, Universität Mainz, D-55099 Mainz, Germany

Received May 9, 2011; E-mail: toyoshima.atsushi@jaea.go.jp

We have investigated the cation-exchange behavior of element 104, rutherfordium (Rf), together with its lighter group-4 homologs Zr and Hf, and the tetravalent pseudo-homolog Th in HF/HNO_3 mixed solution. The results, obtained on a one-atom-at-a-time scale, demonstrate that distribution coefficients (K_d) of Rf in $HF/0.10\,M$ HNO_3 decrease with increasing concentration of the fluoride ion $[F^-]$. This resembles the behavior of the homologs, indicating the consecutive formation of fluorido complexes of Rf. We also measured the K_d values of Rf and the homologs as a function of the hydrogen ion concentration $[H^+]$ in the range of $[F^-] = 5.29 \times 10^{-7}$–$3.17 \times 10^{-6}\,M$. The $\log K_d$ values decrease linearly with an increase of $\log[H^+]$ with slopes between -2.1 and -2.5. This indicates that these elements are likely to form the same chemical compounds: mixture of $[MF]^{3+}$ and $[MF_2]^{2+}$ (M = Rf, Zr, Hf, and Th) in the studied solution. It is also ascertained that the fluorido complex formation of Rf is significantly weaker than that of Zr and Hf, but it is stronger than that of Th.

Chemical characterization of the transactinoid elements with atomic numbers $Z \geq 104$ is an extremely fascinating and challenging subject in modern nuclear and inorganic chemistry.[1–5] A very important and interesting aspect is to clarify chemical properties of these newly synthesized elements at the uppermost end of the Periodic Table and to elucidate the influence of relativistic effects on chemical properties of the heaviest elements.[6,7] The transactinoid elements, however, must be produced at accelerators in heavy-ion-induced nuclear reactions and are available only as short-lived isotopes in quantities of one or a few atoms at a time. Thus, each atom produced decays before a new atom is synthesized. This means that any chemical experiment to be performed must be done on an atom-at-a-time scale. In addition, each available atom should be chemically equilibrated rapidly within its lifetime: typically in the range of one to several tens of seconds. Such restricted experimental conditions make it remarkably difficult to characterize chemical properties of these elements. Usually, chemical experiments with the transactinoid elements are conducted together with their respective homologs in the Periodic Table using partition methods.[1–5] The observed chemical behavior of the transactinoid elements is discussed based on comparative studies with the homologs.

Element 104, rutherfordium (Rf) is the first transactinoid element. As a 6d transition element and member of the seventh row, it is placed in group-4 of the Periodic Table. The first pioneering aqueous-phase separation of Rf, using a cation-exchange chromatography column and the chelating agent α-hydroxyisobutyric acid (α-HiB), was conducted by Silva et al.[8] They clearly demonstrated that the adsorption behavior of the Rf complexes on the resin is entirely different from that of the complexes of trivalent actinoid elements but similar to that of Zr and Hf complexes in group-4. Hulet et al. then revealed that the chloride complexation of Rf is much stronger than that of the trivalent actinoid elements and is similar to that of Hf.[9]

Further attempts to clarify chemical properties of Rf in solution have been made through comparative studies of Rf with its lighter homologs. Fluoride complexation of Rf was studied by several authors as the fluoride ion is a strong

Published on the web August 23, 2011; doi:10.1246/bcsj.20110126

complexing agent for group-4 elements. Kacher et al. reported that the extraction of group-4 elements from 0.5 M hydrofluoric acid (HF) into triisooctylamine (TIOA) follows the sequence Ti > Zr = Hf > Rf,[10] although no quantitative assessment of the extraction yield is made. Subsequent studies using ion-exchange techniques were carried out by Szeglowski et al.,[11] Pfrepper et al.,[12] Schumann et al.,[13] Strub et al.,[14] and Kronenberg et al.[15] A most interesting result concerning the cation- and anion-exchange behavior of Rf in 0.0001 to 1 M HF and 0.1 M HNO_3 mixed solution was observed by Strub et al.; the cation-exchange behavior of Rf was intermediate between those of Zr/Hf and Th, while the anion-exchange behavior of Rf was different from that of the homologs Zr and Hf. Haba et al.[16] and Toyoshima et al.[17,18] then studied the fluoride complexation of Rf through anion-exchange chromatography together with the lighter homologs Zr and Hf in 1.9 to 13.9 M HF and in HF/HNO_3 mixed solutions. These results revealed that the anion-exchange behavior of Rf is remarkably different from that of Zr and Hf, and that the fluoride complexation of Rf is much weaker than that of the homologs. Additionally, the work of Toyoshima et al. provided strong experimental evidence for the formation of the hexafluorido complex of Rf, $[RfF_6]^{2-}$, like $[ZrF_6]^{2-}$ and $[HfF_6]^{2-}$ in the fluoride ion concentrations of 0.0005 to 0.013 M. This enabled a detailed discussion of the interaction between Rf and F^-.[18]

In a previous letter,[19] we reported the cation-exchange behavior of Rf in 0.005 to 0.1 M HF/0.1 M HNO_3 solution and suggested a consecutive fluorido complex formation of Rf like Zr, Hf, and Th. In this paper, new and more precise data on the adsorption of Rf on a cation-exchange resin from 0.005 to 0.1 M HF/0.07 to 0.225 M HNO_3 solution are presented. These results provide a basis to determine the chemical species of Rf on the cation-exchange resin and to discuss the fluoride complexation of Rf by comparing these results with fully relativistic density functional calculations.[20] The cation-exchange chromatographic behavior of the short-lived radioisotopes ^{261}Rf, ^{85}Zr, and ^{169}Hf was investigated using an automated ion exchange separation apparatus coupled with a detection system for α spectroscopy (AIDA). The distribution coefficients (K_d) of Zr, Hf, and Th on cation-exchange resin by a batch method using the long-lived radiotracers ^{88}Zr, ^{175}Hf, and ^{234}Th were also measured to compare with those by the column methods with AIDA. To examine the coordination of NO_3^- to these elements, the variation of the K_d values of these elements was also measured using an electrolyte with a weaker complexing strength, the perchlorate ion (ClO_4^-).

Experimental

Batch Experiments. The carrier-free radiotracers ^{88}Zr (half-life $T_{1/2} = 83.4$ d) and ^{175}Hf ($T_{1/2} = 70.0$ d) were produced via the ^{89}Y(p, $2n$) and ^{175}Lu(p, n) reactions, respectively, using the JAEA tandem accelerator. The irradiated target material was dissolved in concentrated HCl and was fed onto an anion-exchange column (DIAION SA#100, 100–200 mesh, Cl^- form, 4 mm i.d. × 40 mm). After washing the column with concentrated HCl, ^{88}Zr and ^{175}Hf tracers were eluted with 4.0 M HCl. Thorium-234 ($T_{1/2} = 24.10$ d) was used as a tracer and was obtained as the α-decay daughter nuclide of natural ^{238}U. Commercially available $UO_2(NO_3)_2 \cdot 6H_2O$ was dissolved in 9.0 M HCl and was loaded onto the anion-exchange column (DIAION SA#100, 100–200 mesh, Cl^- form, 28 mm i.d. × 300 mm). The effluent was evaporated to dryness, was dissolved in 9.0 M HNO_3, and was fed onto a second anion-exchange column (Dowex 1 × 8, 200–400 mesh, NO_3^- form, 4 mm i.d. × 40 mm). After washing the column with 9.0 M HNO_3, ^{234}Th was eluted with 0.1 M HNO_3. All radiotracers were stored in polypropylene vessels in 0.1 and 2.0 M HNO_3, and 0.1 and 2.0 M $HClO_4$ solutions.

For batch experiments, the cation-exchange resin used was MCI GEL CK08Y, supplied by Mitsubishi Chemical Corporation, a strongly acidic quaternary-amine polymer with a particle size of 20 μm. The resin was stirred five times alternately in 4.0 M HCl and in 4.0 M NaOH solutions and was converted to the hydrogen (H^+) form by washing with 4.0 M HCl solution. Then, the resin was rinsed several times with distilled water and was dried to a constant weight at 110 °C in a vacuum oven. The dried resin was kept in a desiccator. Portions of 10 to 200 mg of CK08Y and 3.0 mL of a HF/HNO_3 or $HF/HClO_4$ mixed solution, containing 50 μL of the tracer solution, were transferred into a polypropylene tube and were shaken for 3 h at 20 °C. After centrifugation, 1.0 mL of the aqueous phase was precisely pipetted into a polyethylene tube. γ-Ray spectra were taken with a Ge detector. As a reference sample, 50 μL of the radiotracer solution was transferred to a separate polyethylene tube and was diluted to 1.0 mL with HF/HNO_3 or $HF/HClO_4$ solution. Control experiments without the CK08Y resin were carried out to evaluate the potential adsorption of radiotracers on the inner wall of the polypropylene tube. The number of ^{88}Zr, ^{175}Hf, and ^{234}Th atoms used for each batch experiment was about 10^{10}. The concentration of HNO_3 and $HClO_4$ solution was determined by titration with Na_2CO_3 solution, while the concentration of HF was determined with standardized NaOH solution.

Online Column Chromatographic Experiments. The nuclide ^{261}Rf ($T_{1/2} = 78$ s), produced in the ^{248}Cm(^{18}O, $5n$) reaction, was used for all chemical studies of Rf. The ^{248}Cm target, with a thickness of 540 μg cm^{-2} and a diameter of 5 mm, was prepared by electrodeposition of $Cm(NO_3)_3$ from 2-propanol onto a Be backing foil with 1.8 mg cm^{-2} thickness. The Cm target contained 39.3%-enriched ^{152}Gd of 32 μg cm^{-2} in thickness to simultaneously produce the short-lived Hf isotope ^{169}Hf ($T_{1/2} = 3.24$ min) through the Gd(^{18}O, xn) reaction. ^{169}Hf was used to determine the chemical yield and the chromatographic behavior of Hf. A 108.4-MeV $^{18}O^{6+}$ beam with an intensity of 250–300 nA (particle), delivered from the JAEA tandem accelerator, passed through a HAVAR vacuum window (1.8 mg cm^{-2}), He cooling gas (0.09 mg cm^{-2}), and the Be target backing, and finally entered the target material at an energy of 94 MeV. At this incident energy, the excitation function for the ^{248}Cm(^{18}O, $5n$) reaction exhibits a maximum cross section of 13 nb.[21] This results in an expected production rate of about two atoms per minute under present conditions.

To investigate the column chromatographic behavior of Zr and Hf on the cation-exchange resin, short-lived ^{85}Zr ($T_{1/2} = 7.86$ min) and ^{169}Hf were simultaneously produced via the ^{nat}Ge(^{18}O, xn) and ^{nat}Gd(^{18}O, xn) reaction (nat: natural isotopic abundance), respectively. The Gd target with 370

$\mu g\,cm^{-2}$ thickness was electrodeposited onto a $2.65\,mg\,cm^{-2}$ Be backing and then, onto the resulting Gd target, $660\,\mu g\,cm^{-2}$ Ge was deposited by vacuum evaporation.

Reaction products recoiling from these targets were stopped in He gas (90 kPa), attached to KCl aerosols generated by sublimation of KCl powder at 640 °C, and were transported through a Teflon capillary (2.0 mm i.d. × 28 m long) by a He/KCl gas-jet to the chemistry laboratory. The transport efficiency of the gas-jet system was estimated to be 30–35%.[21]

Online cation-exchange chromatography was performed with AIDA.[16,18] It consists of a modified automated rapid chemistry apparatus (ARCA) which is a miniaturized computer-controlled high-performance liquid chromatography (HPLC) system[22] and an automated online α-particle detection system.[23] The reaction products, transported by the He/KCl gas-jet system, were deposited on the collection site of AIDA for 130 s. Then the products were dissolved in 250 µL of HF/HNO_3 solution of various concentrations. At a flow rate of $0.7\,mL\,min^{-1}$ this solution was fed onto a chromatographic column (1.6 mm i.d. × 7.0 mm or 1.0 mm i.d. × 3.5 mm) packed with the CK08Y resin. The effluent was collected on a Ta disk as fraction 1 and was evaporated to dryness using hot He or N_2 gas and a halogen heat lamp. Remaining products were stripped from the column with 250 µL of 0.1 M HF/0.1 M HNO_3 at a flow rate of $1.0\,mL\,min^{-1}$. This second effluent was collected on a second Ta disk as fraction 2 and was evaporated to dryness in the same manner. Both disks were automatically transferred to an α-spectrometry station equipped with eight $600\,mm^2$ passivated ion-implanted planar silicon (PIPS) detectors. The chromatographic separation was accomplished within 25 s and the α-particle measurement started 80 and 120 s after aerosol collection for fractions 1 and 2, respectively. Every step of the separation and measurement was controlled by a computer. These separation processes were repeated about 1900 times with AIDA. Counting efficiencies of each detector ranged from 30 to 40% depending on geometric differences of the dried α-sources, and the α-particle energy resolution was 100–200 keV FWHM. All energy signals were registered event by event together with time and detector information. After the α-particle measurement, the 493 keV γ-radiation of ^{169}Hf in every third pair of Ta disks was monitored with Ge detectors to determine the chromatographic behavior of Hf and its chemical yield. The chemical yield of ^{169}Hf, including deposition and dissolution efficiencies of the aerosols, was approximately 60%.

All experiments with ^{85}Zr and ^{169}Hf were conducted prior to those with ^{261}Rf and ^{169}Hf. Reaction products transported by the He/KCl gas-jet method were collected on the deposition site of AIDA for 60 to 180 s. Then, the products were dissolved in a HF/HNO_3 mixed solution and were subsequently loaded onto a cation-exchange column under the same experimental conditions as those with the Rf and Hf experiments. Effluent fractions were consecutively collected in seven polyethylene tubes. Remaining products in the column were stripped with 0.1 M HF/0.1 M HNO_3 and were collected in a separate polyethylene tube. The 416 and 370 keV γ-rays of ^{85}Zr and ^{169}Hf, respectively, in each tube were assayed by γ-ray spectrometry with Ge detectors to obtain elution curves of the homologs. The number of ^{85}Zr and ^{169}Hf atoms used for each online experiment was about 10^6.

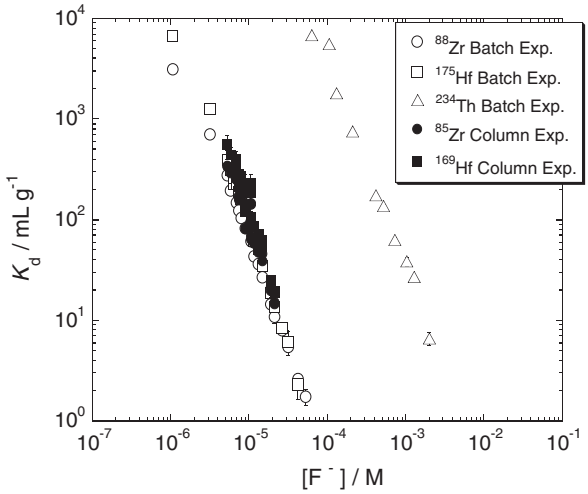

Figure 1. Variation of the distribution coefficients, K_d, of Zr, Hf, and Th on the cation-exchange resin CK08Y in HF/0.10 M HNO_3 as a function of the fluoride ion concentration [F^-]. Open symbols indicate the data obtained in the batch experiments, while solid ones show those in the column experiments.

Results and Discussion

Batch Experiments with ^{88}Zr, ^{175}Hf, and ^{234}Th. The [F^-] Dependence of the Distribution Coefficient: The coefficient, K_d ($mL\,g^{-1}$), for the distribution of these elements between the resin and the solution is expressed using the following equation:

$$K_d = \frac{A_R V_S}{A_S W_R} \quad (1)$$

where A_R and A_S are radioactivities in the resin and the solution, respectively, V_S is the volume of the solution (mL) and W_R the mass of the dry resin (g). As HF is a weak acid, it partially dissociates in aqueous solution. The following equilibria are formed in the HF/HNO_3 mixed solution,

$$H^+ + F^- \rightleftarrows HF \qquad K_1 \quad (2)$$

$$HF + F^- \rightleftarrows HF_2^- \qquad K_2 \quad (3)$$

$$HNO_3 \rightleftarrows H^+ + NO_3^- \quad (4)$$

with the dissociation constants $K_1 = 935\,M^{-1}$ and $K_2 = 3.12\,M^{-1}$ for the dissociation of HF according to eqs 2 and 3, respectively.[24] For the nitric acid, complete dissociation was assumed. On the basis of the law of mass action, equilibrated concentrations were evaluated for each ion in various HF/HNO_3 solutions.

The K_d value dependence of ^{88}Zr, ^{175}Hf, and ^{234}Th on CK08Y as a function of the fluoride ion concentration [F^-] in HF/0.1 M HNO_3 solution is shown in Figure 1 as open symbols: $\log K_d$ vs. $\log[F^-]$. The K_d values of these elements decrease with increasing [F^-]. In Refs. 25–27, this dependence was used to determine the stability constants of fluorido complexes of Zr and Hf which show the consecutive formation of the fluorido complexes. The K_d values of Zr and Hf decrease at lower fluoride ion concentration compared with those of Th.

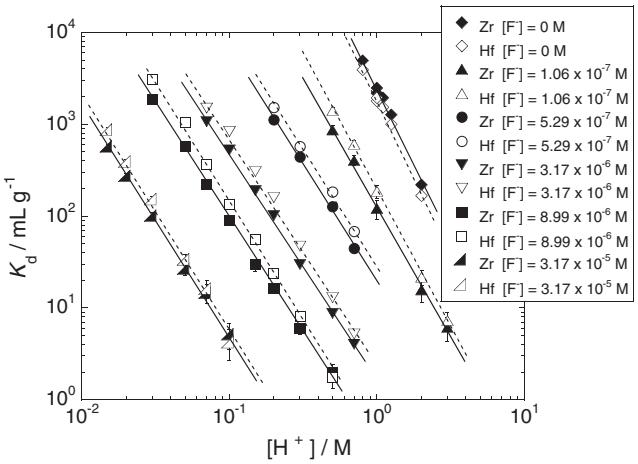

Figure 2. Variation of the K_d values of ^{88}Zr and ^{175}Hf as a function of [H$^+$] at various fluoride ion concentrations [F$^-$] in HF/HNO$_3$ solutions by closed and open symbols, respectively. Solid and dashed lines indicate the least-squares fit to the data of ^{88}Zr and ^{175}Hf, respectively.

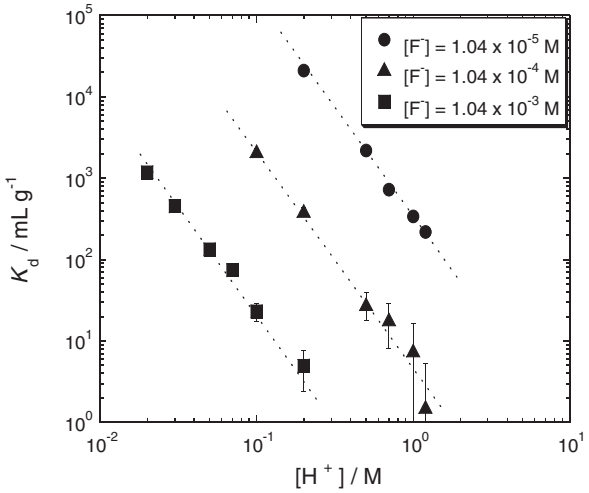

Figure 3. Variation of the K_d values of ^{234}Th as a function of [H$^+$] at various fluoride ion concentrations [F$^-$] in HF/HNO$_3$ solutions. Dotted lines indicate the least-squares fit to the data.

The [H$^+$] Dependence of the Distribution Coefficient: In Figure 2, the variation of K_d values of ^{88}Zr and ^{175}Hf is shown as a function of the hydrogen ion concentration [H$^+$] in $[F^-] = 0\,M$ and $1.06 \times 10^{-7} \leq [F^-] \leq 3.17 \times 10^{-5}\,M$, while that of ^{234}Th at $[F^-] = 1.04 \times 10^{-3}$, 1.04×10^{-4}, and $1.04 \times 10^{-5}\,M$ is plotted against [H$^+$] in Figure 3. The solid and dashed lines in Figure 2 are the results of the least-squares fit to the data of ^{88}Zr and ^{175}Hf, respectively. It is found that the $\log K_d$ values of these elements linearly decrease with an increase of log[H$^+$] with a slope of approximately -2.5. Figure 4a shows, for ^{88}Zr, ^{175}Hf, and ^{234}Th, the variation of the slopes observed in the $\log K_d$ vs. log[H$^+$] plots as a function of [F$^-$]. The slopes for each element are independent of the fluoride ion concentration $[F^-] \geq 5.29 \times 10^{-7}\,M$, i.e., above this limiting value of [F$^-$] the slope remains constant when varying [H$^+$].

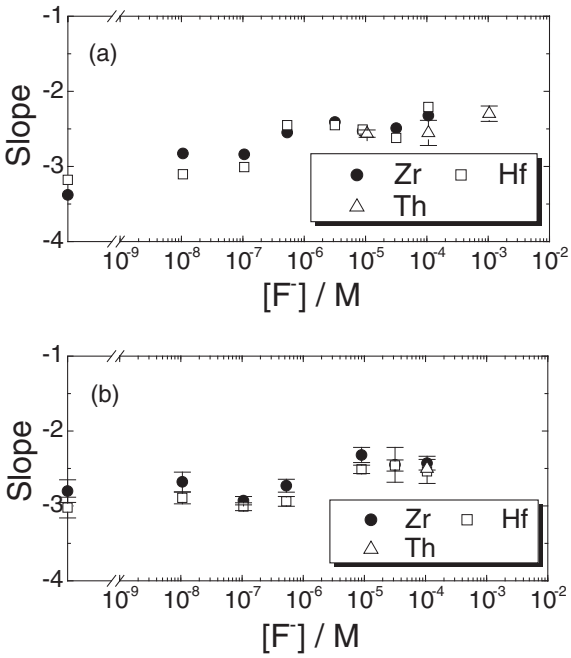

Figure 4. Variation of the slopes for ^{88}Zr, ^{175}Hf, and ^{234}Th in the $\log K_d$ vs. log[H$^+$] plot as a function of [F$^-$]: (a) in HF/HNO$_3$ and (b) in HF/HClO$_4$.

At constant fluoride ion concentration, the cation-exchange behavior of fluorido complexes between the solution and the resin phase is expressed by the following reaction,

$$(4-n)\mathrm{H}^+ + [\mathrm{MF}_n{}^{(4-n)}]_\mathrm{R} \rightleftarrows [(4-n)\mathrm{H}^+]_\mathrm{R} + \mathrm{MF}_n{}^{(4-n)} \quad (5)$$

where n is the number of the coordinated fluoride ions ($n = 1$ to m) to M^{4+} (M = Zr, Hf, and Th) for their dominant species and the subscript R denotes the resin phase. Introducing the selectivity coefficient K,

$$K = \frac{[\mathrm{H}^+]_\mathrm{R}{}^{(4-n)} \cdot [\mathrm{MF}_n{}^{(4-n)}]}{[\mathrm{H}^+]^{(4-n)} \cdot [\mathrm{MF}_n{}^{(4-n)}]_\mathrm{R}} \quad (6)$$

The distribution coefficient K_d for the adsorbed single species is expressed as,

$$K_\mathrm{d} \equiv \frac{[\mathrm{MF}_n{}^{(4-n)}]_\mathrm{R}}{\sum[\mathrm{MF}_n{}^{(4-n)}]} = \frac{\beta_n[\mathrm{F}^-]^n}{K\left(1 + \sum_{i=1}^{m}\beta_i[\mathrm{F}^-]^i\right)}\left(\frac{[\mathrm{H}^+]_\mathrm{R}}{[\mathrm{H}^+]}\right)^{(4-n)} \quad (7)$$

where β_i ($i = 1$ to m) are stability constants of the $MF_n{}^{(4-n)}$ species represented as $\beta = \prod_{i=1}^{m} K_i$ with formation constants K_i. In the tracer scale experiment, $[H^+]_R$ and K could be assumed to be constant. Then taking the logarithm of the both sides of eq 7, one obtains,

$$\log K_\mathrm{d} \propto -(4-n)\log[\mathrm{H}^+] \quad (8)$$

Thus, from the slope in the $\log K_d$ vs. log[H$^+$] plot, we can evaluate the number of the coordinated fluoride ions to the metal cation on the resin.

Under the present dilute [F$^-$] conditions, coordination of the nitrate ion NO_3^- to M^{4+} should be also taken into account. To examine the coordination of NO_3^-, the K_d-value variations of ^{88}Zr, ^{175}Hf, and ^{234}Th were measured using the perchlorate ion,

ClO_4^-, as a much weaker coordinating support electrolyte. The slopes obtained in the $HF/HClO_4$ solution are depicted in Figure 4b as a function of $[F^-]$. It is found that all slopes from the experiments with $[F^-] > 10^{-5}$ M are the same as those observed in HF/HNO_3. This means that in the studied region of $[F^-] > 10^{-5}$ M, no significant effect of the NO_3^- ion was observed. The contribution of hydrolysis is considered to be negligible based on the reported stability constants of hydrolysis products and the fluoride complexes as well as the concentration of F^- and OH^- ions in this experiment.[20] Thus, the number of the coordinated fluoride ions on the cation-exchange resin is deduced to be about 1.5; thus, $[MF]^{3+}$ and $[MF_2]^{2+}$ are dominant species on the cation-exchange resin.

Connick and McVey[28] studied the kind of Zr complexes in acidic solutions containing HF. They reported that the average number of fluoride ions per zirconium ion is one in 2×10^{-5} M HF with $[H^+] = 2.0$ M which leads to $[F^-] = 1.06 \times 10^{-7}$ M. As shown in Figures 4a and 4b, the slopes of -3 in the $\log K_d$ vs. $\log[H^+]$ plot are obtained at around $[F^-] = 10^{-7}$ M. This indicates that $[MF]^{3+}$ is predominantly adsorbed on the resin. This is consistent with the result obtained by Connick and McVey.[28]

In the pure HNO_3 and/or $HClO_4$ solutions ($[F^-] = 0$ M), hydrolysis is expected to occur.[28] The slope of about -3 at $[F^-] = 0$ M probably reflects the fact that $[M(OH)]^{3+}$ is the predominant species adsorbed on the resin.

Online Chromatographic Experiments with ^{85}Zr, ^{169}Hf, and ^{261}Rf. Figures 5a and 5b show typical elution curves of ^{85}Zr and ^{169}Hf. The curves in $[F^-] = 6.88 \times 10^{-6}$ and 1.06×10^{-5} M/0.1 M HNO_3 obtained with the 1.0 mm i.d. × 3.5 mm column are depicted in Figure 5a, while those in $[F^-] = 1.16 \times 10^{-5}$ and 1.90×10^{-5} M/0.1 M HNO_3 with the 1.6 mm i.d. × 7.0 mm column are in Figure 5b. The flow rate was 0.7 mL min^{-1} for both columns. According to the Glueckauf model of chromatography[29] that is based on the theoretical plate concept assuming a continuous flow and local equilibrium, the eluted radioactivity per unit volume $A(v)$ with the effluent volume v is represented by the following equation:

$$A(v) = A_{max} \exp\left\{-\frac{N}{2}\frac{(V_{max} - v)^2}{V_{max} v}\right\} \quad (9)$$

where parameters A_{max}, N, and V_{max} are the maximum peak height, the number of theoretical plates, and the effluent volume (mL) at the maximum peak height of the elution curve, respectively. Values of V_{max} and v were corrected for column dead volumes: 42 and 21 μL for the 1.6 mm i.d. × 7.0 mm and 1.0 mm i.d. × 3.5 mm columns, respectively. Results of the fits applying eq 9 are drawn as solid lines and dashed lines for ^{85}Zr and ^{169}Hf, respectively. For each condition, good agreement is obtained between the experimental data and the calculation. The calculated number of theoretical plates N is 7.3 ± 2.8 and 3.0 ± 1.4 for the 1.6 mm i.d. × 7.0 mm and 1.0 mm i.d. × 3.5 mm columns, respectively.

In a column chromatographic system, the K_d value is expressed as

$$K_d = \frac{V_{max}}{W_R} \quad (10)$$

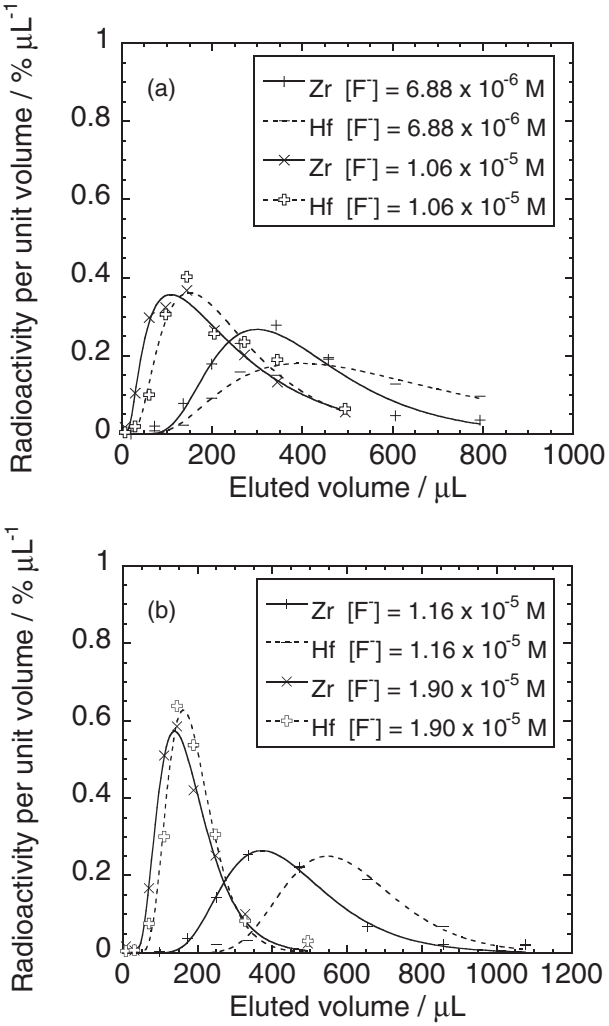

Figure 5. Typical elution curves of ^{85}Zr and ^{169}Hf using (a) the 1.0 mm i.d. × 3.5 mm column and (b) the 1.6 mm i.d. × 7.0 mm column in $HF/0.1$ M HNO_3 solutions as eluents. Solid and dashed curves represent the fit with the Glueckauf model for ^{85}Zr and ^{169}Hf, respectively.

where W_R is the mass of dry resin (g). The average W_R value was measured to be 6.4 ± 0.4 and 1.2 ± 0.2 mg for the 1.6 mm i.d. × 7.0 mm and 1.0 mm i.d. × 3.5 mm columns, respectively. K_d values obtained with the column chromatographic method are also plotted in Figure 1 by closed symbols. Both sets of K_d values, the ones obtained by the batch experiments and one derived from the column chromatographic separations agree well with each other. This indicates that the chemical reactions reached equilibrium for all column separations.

Results of the experiments with Rf are summarized in Tables 1 and 2. A total of 1896 cycles of the cation-exchange experiments were conducted and 237 α-particles from the decays of ^{261}Rf ($E_\alpha = 8.28$ MeV)[30] and its daughter nuclide ^{257}No ($E_\alpha = 8.22$ and 8.32 MeV)[31] were observed in the α-particle energy range of 8.00–8.36 MeV. This includes 41 time-correlated α pairs of ^{261}Rf and ^{257}No. Typical α-energy spectra of samples prepared from the two effluents, fraction 1 (2.50×10^{-2} M $HF/0.10$ M HNO_3) and fraction 2 (stripping solution: 0.10 M $HF/0.10$ M HNO_3) from 278 cycles are shown

Table 1. Summary of Online Experiments with Rf in HF/0.10 M HNO_3 Solutions[a)]

[HF]/M	$[F^-]$/M	Beam dose /$\times 10^{17}$	Number of cycles of the experiment	α-Count in fraction 1		α-Count in fraction 2		%ads of ^{261}Rf /%	K_d of ^{261}Rf /mL g^{-1}
				α	α–α	α	α–α		
5.00×10^{-3}	5.29×10^{-5}	0.497	251	2	0	23	2	95^{+3}_{-5}	350^{+120}_{-70}
1.00×10^{-2}	1.06×10^{-4}	1.02	429	32	4	12	0	33^{+8}_{-7}	78^{+21}_{-16}
1.30×10^{-2}	1.37×10^{-4}	0.254	108	7	1	3	0	36^{+17}_{-13}	82^{+44}_{-30}
2.50×10^{-2}	2.63×10^{-4}	0.667	278	25	5	17	4	48^{+8}_{-7}	21^{+3}_{-2}
4.00×10^{-2}	4.20×10^{-4}	0.193	82	16	4	0	0	0	<15
1.00×10^{-1}	1.04×10^{-3}	0.257	179	10	2	0	0	0	<15

a) The upper three lines represent data obtained with 1.0 mm i.d. × 3.5 mm columns, while the lower three lines are those with 1.6 mm i.d. × 7.0 mm columns.

Table 2. Summary of Online Experiments with Rf in HF/HNO_3 Solutions at $[F^-] = 1.06 \times 10^{-4}$ M[a)]

[HF]/M	$[H^+]$/M	Beam dose /$\times 10^{17}$	Number of cycles of the experiment	α-Count in fraction 1		α-Count in fraction 2		%ads of ^{261}Rf /%	K_d of ^{261}Rf /mL g^{-1}
				α	α–α	α	α–α		
7.06×10^{-2}	0.07	0.507	215	3	0	22	5	92^{+4}_{-6}	290^{+60}_{-50}
1.00×10^{-2}	0.1	1.02	429	32	4	12	0	33^{+8}_{-7}	68^{+19}_{-17}
1.25×10^{-2}	0.125	0.280	119	13	3	3	0	21^{+9}_{-7}	39^{+22}_{-20}
1.75×10^{-2}	0.175	0.287	119	1	0	20	3	97^{+2}_{-5}	>42
2.24×10^{-2}	0.225	0.394	166	17	5	11	3	47^{+10}_{-9}	21^{+3}_{-2}

a) The upper three lines represent data obtained with 1.0 mm i.d. × 3.5 mm columns, while the lower two lines are those with 1.6 mm i.d. × 7.0 mm columns.

in Figure 6. The expected event ratio between α-singles and α–α correlations was calculated to be 5 by taking into account the counting efficiency of the detector ($\approx 35\%$) and the growth and decay of ^{261}Rf and ^{257}No. The contribution of α-decays from those of ^{257}No which were formed from ^{261}Rf during the collection period before the cation-exchange separation started was also taken into account on the basis of standard equations of growth and decay. It was assumed that the divalent state of ^{257}No was strongly adsorbed on the cation-exchange resin[32] and was not eluted with any solutions used in this experiment. The observed ratio of 4.8 ± 1.7 for α-singles to α–α-correlations is consistent with the estimated value within the counting statistics. The average background, determined in a long counting interval after the experiment, was 3.2×10^{-6} counts s^{-1} for each detector in the α-energy range of interest. The asymmetric error limits of the %ads values of ^{261}Rf were evaluated from the counting statistics of the observed α events based on the 68% confidence intervals for Poisson distributed variables.[33]

From the radioactive decays A_1 and A_2 observed in fractions 1 and 2, respectively, the adsorption probability (%ads) on the resin was evaluated using the relation: $\%\text{ads} = 100 \times A_2/(A_1 + A_2)$. Proper corrections were made for the radioactive decay losses and for the background. K_d values of Rf were evaluated from the percent adsorption values (%ads) at a fixed volume of the effluent. It was assumed that reaction kinetics in the fluorido complex formation and in all cation-exchange processes of Rf was as fast as those for Zr and Hf: see Refs. 16–18 for a further description. Figures 7a and 7b depict variations of %ads values of Zr and Hf on the cation-exchange resin CK08Y obtained with the columns of 1.6 mm i.d. × 7.0 mm and 1.0 mm i.d. × 3.5 mm, respectively, as a function of K_d obtained from the batch experiments with the same kind of solution. All %ads values smoothly correlate with K_d. The correlation between the %ads values and the K_d values was fitted by the following equation containing the free parameters a, b, and c,

$$\%\text{ads} = 100 \times \exp\{-a \exp[-b(K_d - c)]\} \quad (11)$$

The fitted values based on eq 11 are shown as solid lines in Figures 7a and 7b. Thus, %ads values of Rf from the column separations can be transformed into K_d values using this relationship.

In Figure 8, the obtained K_d values of Rf are plotted as a function of $[F^-]$ together with those of Zr, Hf, and Th in HF/0.1 M HNO_3. The arrows indicate the upper limit values for K_d of Rf. It is clearly found that the K_d values of Rf also decrease with an increase of $[F^-]$ being between those of Zr/Hf and Th, clearly confirming the previous results.[14,19] These results indicate that the cationic fluorido complexes of Rf adsorbed onto the resin decrease with increasing $[F^-]$. In our previous anion-exchange study,[18] the K_d values of Rf in HF/HNO_3 solution increased in the range of $5 \times 10^{-4}\,\text{M} \leq [F^-] \leq 1.3 \times 10^{-2}\,\text{M}$. This was interpreted as the consecutive formation of fluorido complexes of Rf as well as the adsorption of the anionic hexafluorido complex $[RfF_6]^{2-}$ on the anion-exchange resin. The present decreasing feature of the K_d values of Rf as an increase of $[F^-]$ further verifies the consecutive formation of its fluorido complexes; cationic fluorido complexes of Rf change to neutral and anionic species with an increase of $[F^-]$.

The K_d values of Rf as a function of $[H^+]$ are depicted in Figure 9 together with those of Zr, Hf, and Th. These data were obtained at $[F^-] = 1.06 \times 10^{-4}$ M. The arrow shows the lower

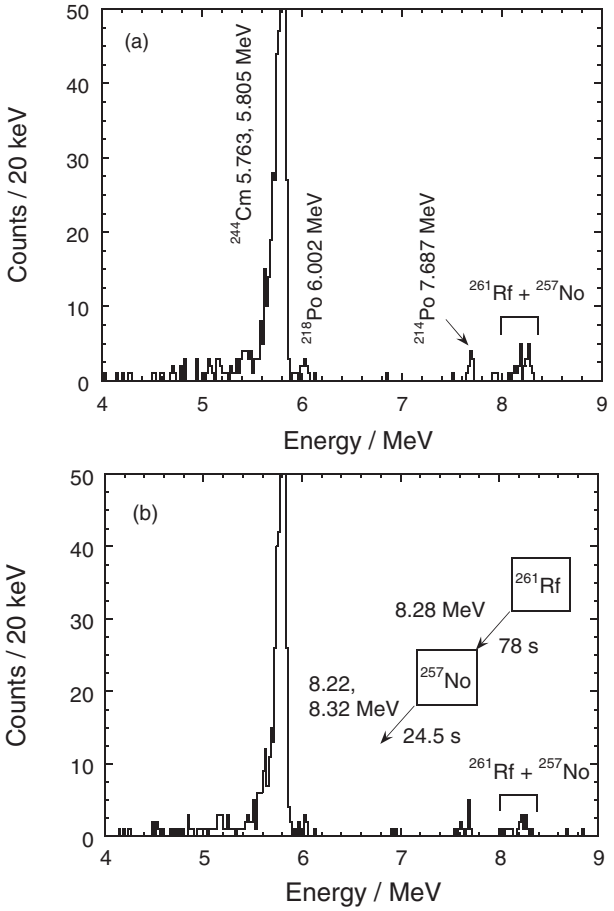

Figure 6. Typical *a*-particle spectra of the samples prepared from the two effluents, (a) fraction 1 (2.50×10^{-2} M HF/0.10 M HNO_3) and (b) fraction 2 (0.10 M HF/0.10 M HNO_3).

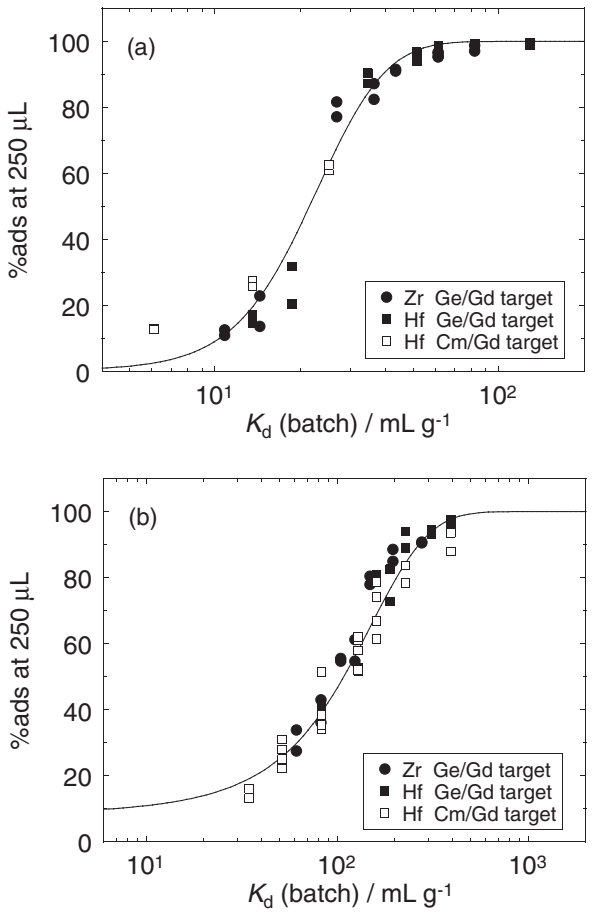

Figure 7. Percent adsorption values, %ads, of Zr and Hf on the cation-exchange resin CK08Y obtained with the columns of (a) 1.6 mm i.d. × 7.0 mm and (b) 1.0 mm i.d. × 3.5 mm as a function of the distribution coefficient K_d obtained in the separate batch experiments with an identical resin and liquid phases.

limit. It is found that $\log K_d$ of Rf also linearly decreases with increasing $\log[H^+]$. As already mentioned, cationic fluorido complexes of these elements are replaced by H^+ ions acting as a counter ion on the cation-exchange site and the slope in the $\log K_d$ vs. $\log[H^+]$ plot reflects the number of the coordinated fluoride ions to the metal cation on the resin.

From the data shown in Figure 9, the slopes from -2.2 ± 0.5 are obtained for Rf at $[F^-] = 1.06 \times 10^{-4}$ M. This indicates that the number of the coordinated fluoride ions is 1 and 2. Under the present conditions, both species $[RfF]^{3+}$ and $[RfF_2]^{2+}$ are most likely those which are present on the resin, similar to those assumed for Zr, Hf, and Th. This means that the chemical form of cationic fluorido complexes of Rf, Zr, Hf, and Th are the same on the cation-exchange resin in the studied $[F^-]$ region.

Based on these results, it is ascertained that the fluoride complexation of Rf is significantly weaker than that of Zr and Hf, but it is stronger than the complexation of Th.

Theoretical Interpretation of Fluoride Complexation of Rf. The observed K_d sequence of Zr ≤ Hf < Rf among the group-4 complexes is in full agreement with that predicted theoretically in Ref. 20 where free energy changes of the complex formation reactions were determined on the basis of fully relativistic density functional theory calculations of

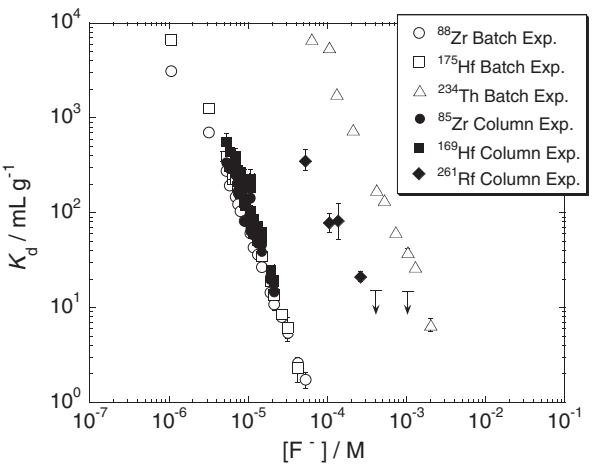

Figure 8. Distribution coefficients, K_d, of Rf, Zr, Hf, and Th between the cation-exchange resin CK08Y and 0.10 M HNO_3 plotted as a function of $[F^-]$. Solid symbols show the data taken from the online column experiments.

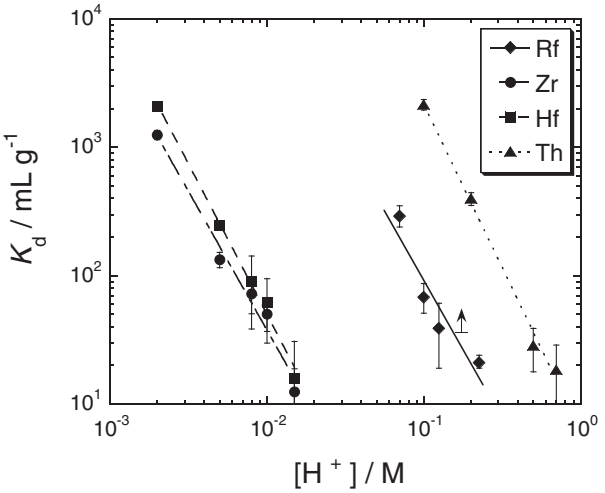

Figure 9. Distribution coefficients, K_d, of Rf, Zr, Hf, and Th between the cation-exchange resin CK08Y and a HF/HNO_3 solution at $[F^-] = 1.06 \times 10^{-4}$ M plotted as a function of $[H^+]$. Solid, dash-dotted, dashed, and dotted lines are the least-squares fits to the data of Rf, Zr, Hf, and Th, respectively.

various hydrated and hydrolized fluorido complexes of Zr, Hf, and Rf. It was shown (see Table 8 in Ref. 20) that at lower HF concentrations and 0.1 M HNO_3, the complex formation occurs preferentially from hydrolyzed species. The strength of formed complexes is predicted as $Zr \geq Hf > Rf$. From this, the following trend in K_d values results: $Zr \leq Hf < Rf$.

It was also shown in Ref. 20 that the electrostatic interaction plays a dominant role in complex formation energies, though it should be determined on the basis of real electronic density distribution obtained as a result of fully relativistic calculations. Due to a predominant electrostatic interaction, a correlation between crystallographic ionic radii (IR)[34] and the strengths of the formed complexes appears quite natural. Ionic radii of the group-4 elements with the coordination number of 6 are: Zr (72 pm)[34] $\approx$ Hf (71 pm)[34] $<$ Rf (76 pm)[7] $\ll$ Th (94 pm).[34] In this particular case, this nicely correlates with the sequence in complex formation $Zr \approx Hf > Rf > Th$. Thus, in agreement with the theory, it is shown experimentally that the formation of positively charged fluorido complexes of Rf is weaker than that of Zr and Hf and stronger than that of Th.

Conclusion

The K_d values of Rf were determined from HF/HNO_3 solution on the cation-exchange resin together with those of the homologs Zr and Hf and the tetravalent pseudo-homolog Th. The result clearly demonstrated the successive fluorido complex formation of Rf. It was also found that the same chemical species $[MF]^{3+}/[MF_2]^{2+}$ (M = Rf, Zr, Hf, and Th) of Rf and its homologs are present and adsorbed on the cation-exchange resin. The order of the adsorption strength on the cation-exchange resin was $Zr \leq Hf < Rf < Th$. The experimentally obtained sequence of the fluoride complexation correlated with the inverse order of the ionic radii. This can be explained on the basis a predominant electrostatic interaction of the tetravalent group-4 elements and Th as the pseudo group-4 element with the fluoride ion F^-. The present result indicated that the ionic radius of Rf^{4+} is in between those of Zr^{4+}/Hf^{4+} and Th^{4+}.

The authors express their gratitude to the crew of the JAEA tandem accelerator for their invaluable assistance in the course of these experiments. This work was supported in part by the JAEA–University Collaboration Research Project and the Program on the Scientific Cooperation between JAEA and GSI in Research and Development in the Field of Ion Beam Application.

References

1 *The Chemistry of Superheavy Elements*, ed. by M. Schädel, Kluwer, Dordrecht, **2003**.
2 J. V. Kratz, *Pure Appl. Chem.* **2003**, *75*, 103.
3 J. V. Kratz, in *Elements and Isotopes: Formation, Transformation, Distribution* in *Handbook of Nuclear Chemistry*, ed. by A. Vértes, S. Nagy, Z. Klencsár, Kluwer, Dordrecht, **2003**, Vol. 2, pp. 323–395.
4 M. Schädel, *Angew. Chem., Int. Ed.* **2006**, *45*, 368.
5 D. C. Hoffman, D. M. Lee, V. Pershina, in *The Chemistry of the Actinide and Transactinide Elements*, 3rd ed., ed. by L. R. Morss, N. M. Edelstein, J. Fuger, Springer, Dordrecht, **2006**, Vol. 3, pp. 1652–1752.
6 V. Pershina, *Chem. Rev.* **1996**, *96*, 1977.
7 V. Pershina, in *The Chemistry of Superheavy Elements*, ed. by M. Schädel, Kluwer, Dordrecht, **2003**, Chap. 2, pp. 31–94.
8 R. Silva, J. Harris, M. Nurmia, K. Eskola, A. Ghiorso, *Inorg. Nucl. Chem. Lett.* **1970**, *6*, 871.
9 E. K. Hulet, R. W. Lougheed, J. F. Wild, J. H. Landrum, J. M. Nitschke, A. Ghiorso, *J. Inorg. Nucl. Chem.* **1980**, *42*, 79.
10 C. D. Kacher, K. E. Gregorich, D. M. Lee, Y. Watanabe, B. Kandkhodayan, B. Wierczinski, M. R. Lane, E. R. Sywester, D. A. Keeney, M. Hendricks, D. C. Hoffman, *Radiochim. Acta* **1996**, *75*, 135.
11 Z. Szeglowski, H. Bruchertseifer, V. P. Domanov, B. Gleisberg, L. J. Guseva, M. Hussonois, G. S. Tikhomirova, I. Zvara, Y. T. Oganessian, *Radiochim. Acta* **1990**, *51*, 71.
12 G. Pfrepper, R. Pfrepper, D. Krauss, A. B. Yakushev, S. N. Timokhin, I. Zvara, *Radiochim. Acta* **1998**, *80*, 7.
13 D. Schumann, H. Nitsche, S. Taut, D. T. Jost, H. W. Gäggeler, A. B. Yakushev, G. V. Buklanov, V. P. Domanov, D. T. Lien, B. Kubica, R. Misiak, Z. Szeglowski, *J. Alloys Compd.* **1998**, *271–273*, 307.
14 E. Strub, J. V. Kratz, A. Kronenberg, A. Nähler, P. Thörle, S. Zauner, W. Brüchle, E. Jäger, M. Schädel, B. Schausten, *Radiochim. Acta* **2000**, *88*, 265.
15 A. Kronenberg, K. Eberhardt, J. V. Kratz, P. K. Mohapatra, A. Nähler, P. Thörle, W. Brüchle, M. Schädel, A. Türler, *Radiochim. Acta* **2004**, *92*, 379.
16 H. Haba, K. Tsukada, M. Asai, A. Toyoshima, K. Akiyama, I. Nishinaka, M. Hirata, T. Yaita, S. Ichikawa, Y. Nagame, K. Yasuda, Y. Miyamoto, T. Kaneko, S. Goto, S. Ono, T. Hirai, H. Kudo, M. Shigekawa, A. Shinohara, Y. Oura, H. Nakahara, K. Sueki, H. Kikunaga, N. Kinoshita, N. Tsuruga, A. Yokoyama, M. Sakama, S. Enomoto, M. Schädel, W. Brüchle, J. V. Kratz, *J. Am. Chem. Soc.* **2004**, *126*, 5219.
17 A. Toyoshima, H. Haba, K. Tsukada, M. Asai, K. Akiyama, I. Nishinaka, Y. Nagame, D. Saika, K. Matsuo, W. Sato, A. Shinohara, H. Ishizu, M. Ito, J. Saito, S. Goto, H. Kudo, H.

Kikunaga, N. Kinoshita, C. Kato, A. Yokoyama, K. Sueki, *J. Nucl. Radiochem. Sci.* **2004**, *5*, 45.

18 A. Toyoshima, H. Haba, K. Tsukada, M. Asai, K. Akiyama, S. Goto, Y. Ishii, I. Nishinaka, T. K. Sato, Y. Nagame, W. Sato, Y. Tani, H. Hasegawa, K. Matsuo, D. Saika, Y. Kitamoto, A. Shinohara, M. Ito, J. Saito, H. Kudo, A. Yokoyama, M. Sakama, K. Sueki, Y. Oura, H. Nakahara, M. Schädel, W. Brüchle, J. V. Kratz, *Radiochim. Acta* **2008**, *96*, 125.

19 Y. Ishii, A. Toyoshima, K. Tsukada, M. Asai, H. Toume, I. Nishinaka, Y. Nagame, S. Miyashita, T. Mori, H. Suganuma, H. Haba, M. Sakamaki, S.-i. Goto, H. Kudo, K. Akiyama, Y. Oura, H. Nakahara, Y. Tashiro, A. Shinohara, M. Schädel, W. Brüchle, V. Pershina, J. V. Kratz, *Chem. Lett.* **2008**, *37*, 288.

20 V. Pershina, D. Trubert, C. L. Naour, J. V. Kratz, *Radiochim. Acta* **2002**, *90*, 869.

21 Y. Nagame, M. Asai, H. Haba, S. Goto, K. Tsukada, I. Nishinaka, K. Nishio, S. Ichikawa, A. Toyoshima, K. Akiyama, H. Nakahara, M. Sakama, M. Schädel, J. V. Kratz, H. W. Gäggeler, A. Türler, *J. Nucl. Radiochem. Sci.* **2002**, *3*, 85.

22 M. Schädel, W. Brüchle, E. Jäger, E. Schimpf, J. V. Kratz, U. W. Scherer, H. P. Zimmermann, *Radiochim. Acta* **1989**, *48*, 171.

23 Y. Nagame, K. Tsukada, M. Asai, A. Toyoshima, K. Akiyama, Y. Ishii, T. Kaneko-Sato, M. Hirata, I. Nishinaka, S. Ichikawa, H. Haba, S. Enomoto, *Radiochim. Acta* **2005**, *93*, 519.

24 M. Plaisance, R. Guillaumont, *Radiochim. Acta* **1969**, *12*, 32.

25 E. L. Zebroski, H. W. Alter, F. K. Heumann, *J. Am. Chem. Soc.* **1951**, *73*, 5646.

26 S. Ahrland, D. Karipides, B. Norén, *Acta Chem. Scand.* **1963**, *17*, 411.

27 B. Norén, *Acta Chem. Scand.* **1967**, *21*, 2449.

28 R. E. Connick, W. H. McVey, *J. Am. Chem. Soc.* **1949**, *71*, 3182.

29 E. Glueckauf, *Trans. Faraday Soc.* **1955**, *51*, 34.

30 *Table of Isotopes*, 8th ed., ed. by R. B. Firestone, V. S. Shirley, John Wiley & Sons, Inc., New York, **1996**.

31 M. Asai, K. Tsukada, M. Sakama, S. Ichikawa, T. Ishii, Y. Nagame, I. Nishinaka, K. Akiyama, A. Osa, Y. Oura, K. Sueki, M. Shibata, *Phys. Rev. Lett.* **2005**, *95*, 102502.

32 J. Maly, T. Sikkeland, R. Silva, A. Ghiorso, *Science* **1968**, *160*, 1114.

33 W. Brüchle, *Radiochim. Acta* **2003**, *91*, 71.

34 R. D. Shannon, *Acta Crystallogr., Sect. A* **1976**, *32*, 751.